Second International Symposium on Marine Propulsors
smp'11, Hamburg, Germany, June 2011

Numerical Design and Experimental Verification of a RIM-Driven Thruster*

Alexey Yu. Yakovlev, Marat A. Sokolov, Nikolay V. Marinich [1]

[1]Krylov Shipbuilding Research Institute (KSRI), St.Petersburg, Russia

ABSTRACT

This paper presents the results of a design and experimental verification of RIM-driven thruster blading system. The propeller was designed by means of direct blade pitch optimization method. Blade camber was set to zero for symmetric port and starboard thruster performance. The strength analysis of blading system under design was carried out and cavitation characteristics were estimated. For verification of the design, a thruster model of tunnel type was manufactured. This model was tested in the deep-water towing tank of the Krylov Shipbuilding Research Institute.

Keywords

RIM-driven propeller, thruster, design, experiment

1 INTRODUCTION

Thrusters with RIM-driven propellers have been known for a long time. They were used, e.g., for the USSR ships *Valeriy Chkalov* and *Rodina*, built in the middle of 20th century in Germany (Lebedev 1969). However, only in recent years have such thrusters come into wide use. Primarily, this has to do with the modern electric motor technologies. It is now possible to build reliable RIM-driven thrusters featuring a number of hydrodynamic and operating advantages over conventional types of thrusters.

Advantages offered by the use of a RIM-driven propeller in thruster unit include:

- Reduced pressure head losses and more uniform wake in propeller disk due to elimination of struts and pod in thruster channel.
- Reduction in thruster-induced noise and vibration due to flow equalization in front of the propeller and elimination of tip vortices in wake of propeller blades.
- No risk of cable entrapment for propeller shaft in case of hubless propeller design.
- No loss of energy due to gap between propeller blade and thruster channel wall.

The issues of design, calculation and experimental investigation of thrusters are addressed in reference with Lebedev et al (1969). The studies on waterjet propulsors (Papir 1970, Kulikov & Khramkin 1965) are also closely related to this subject.

The theory presented in these papers can be successfully applied to the design of thrusters with RIM-driven propeller because specific features of its hydrodynamic configuration have no principal effect on the main calculation procedures. Recent publications (Kinnas et al 2009) confirm this statement, since the modern computation techniques are integrated into the traditional pattern of calculations.

2 STATEMENT OF PROBLEM

The thruster performance is essentially dependent on the type on the tunnel shape and, in particular, on the arrangement of propeller within the tunnel. In our case, the simplest and a widely-used tunnel design is a straight pipe smoothly joined to the ship hull on both sides. In a general case, the thruster can be assumed to have a propeller or a pair of counter-rotating propellers including CP propeller option. Additionally, the thruster can be fitted with flow guide vane systems. Propellers are traditionally fitted to vertical shafts. In the case under consideration, a single propeller is placed in a tunnel. The pod is eliminated due to RIM-driven design because the propeller is rotated using the RIM drive, which is also used to fix propeller blades. Two propeller design options are considered, viz., hub-type propeller design and hubless propeller design. Since the thruster is to have equally efficient port and starboard performance, it was decided to design a propeller with symmetrical blade shape. Usually, the main operating mode for thruster is the bollard pull mode. In the case under consideration, the design advance ratio is assumed equal to J=0.13, which is practically very close to the bollard-pull condition. The formulated requirements determined the type of thruster under study.

* This project was sponsored by the Grant Council of the Russian Federation President (Grant MD-8150.2010.8).

The purpose of studies was to examine the feasibility of developing a successful RIM-driven propeller (hub-type or hubless design options) for thruster unit.

3 PROPULSION SYSTEM DESIGN

3.1 Thruster design

Thrusters can be designed with fixed-pitch propellers (FPP) or controllable pitch propellers (CPP) or counter-rotating propellers. This paper considers only a case of thruster with single FPP. The main operating mode is assumed to be the bollard-pull mode. The design process includes two phases: estimation of pressure head losses in the thruster channel; and determination of propeller geometry. The pressure head losses are commonly estimated using relations of individual component losses versus a number of geometric and hydrodynamic parameters of thruster. These relations can be obtained by generalization of extensive experimental data (Idelchik 1992). In the non-dimensional form, these losses can be expressed in terms of resistance coefficients:

$$\xi = \frac{\Delta p}{\rho \frac{V_S^2}{2}} = \xi_I + \xi_L + \xi_M + \xi_P \qquad (1)$$

where the following resistance coefficients are introduced: ξ_I – at the thruster channel entry, ξ_L – friction over the channel length, ξ_M – grids at the channel entry and exit, ξ_P – propeller pod, Δp – pressure difference due to energy losses, V_S – velocity in thruster channel, ρ - water density.

Energy losses at the entry of thruster channel depend on the shapes of water intake edges and inclination angle of hull sides. Losses due to friction over the channel length are calculated by a traditional method using Blasius formula (Idelchik 1992). Losses due to protective grids are represented by a function of grid blockage coefficient (there were no such losses in our case). Losses due to pod depend on the pod length and diameter (for streamlined pods these losses are limited).

Based on the estimated pressure head losses, the operating mode of propeller in tunnel is to be determined. For this purpose the waterjet theory is applied (Rusetskiy & Mavlyudov 2009) to find the propeller design advance ratio, which is determined based on the internal velocity, as well as the required thrust coefficient of propeller. Then, in accordance with the prescribed procedures, the propeller is to be designed for the given mode using available propeller diagrams for the thruster. However, it is impossible to use the above-said diagrams for RIM-driven propellers and a special-purpose method is to be used for calculation of propeller in tunnel.

3.2 Calculation of propeller in tunnel

In this study the propeller in tunnel is calculated using the method (Vasiliev & Yakovlev 2001) based on calculation of flow around 2D foil lattices. In spite of using a simplified mathematical model, this method calculates with sufficient accuracy the thrust coefficient and efficiency as well as the pressure distribution over blade for a wide range of operating conditions. Further, the following expressions of characteristics will be used:

$$K_T = \frac{T}{\rho n^2 D^4}$$

$$K_Q = \frac{Q}{\rho n^2 D^5}$$

$$\eta = \frac{K_T}{K_Q} \cdot \frac{J}{2\pi} \qquad (2)$$

$$J = \frac{V}{nD}$$

$$J_S = \frac{V_S}{nD}$$

where T – propeller thrust, Q – propeller axial torque, n - number of revolutions, D – propeller diameter, V - inflow velocity, V_S – mean velocity in tunnel, η - propeller efficiency , K_T – propeller thrust coefficient, K_Q – propeller torque coefficient, J – propeller advance ratio, J_S – propeller internal advance ratio.

The accuracy of calculations by the method (Vasiliev & Yakovlev 2001) can be assessed using a case of OD-10 axial pump (Papir 1970). Fig. 1 compares calculations and experimentally obtained thrust versus advance ratio for this pump. Since the pump may have different blade pitch angle settings Φ, Fig. 1 presents the results obtained for a number of pitch angles. Calculations showed satisfactory agreement with experimental data for a wide range of pitch angles.

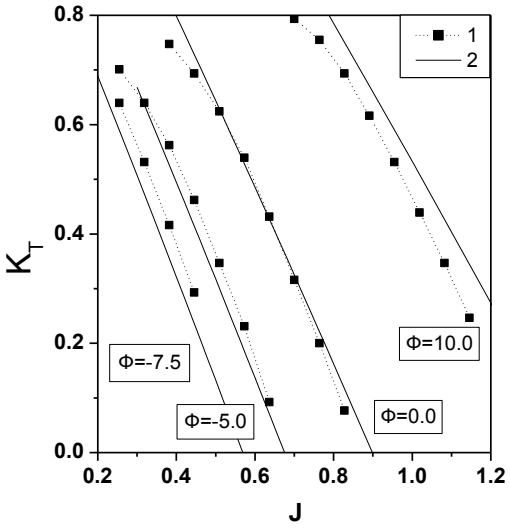

Figure 1: Comparison of calculated and experimentally obtained characteristics of the OD-10 pump at different angles of blade pitch change Φ (deg).
1 – experiment, 2 – analytical method (Vasiliev & Yakovlev 2001).

3.3 Propeller design

The method presented above provides solution to the direct problem, i.e., estimation of propeller characteristics

in tunnel. For propeller design it is required to solve a so-called inverse problem, i.e., to determine the propeller blade shape for given characteristics. From the mathematical point of view, the inverse problem can be quite simply formalized and reduced to multiple solution of the direct problem. This approach is called "direct optimization of propeller" in order to differentiate it from more traditional design methods.

Strictly speaking, it is required to solve an optimization problem including the objective function and several constraints:

$$\begin{cases} 1-\eta(H)+k\cdot\max\limits_{r,\xi}\left|C_P(H)\right|\to\min \\ K_T(H,J_{S0})=K_{T0} \\ H(r)>H_{\min}(r) \\ f=0 \end{cases} \quad (3)$$

where $H=H(r)$ - function describing blade pitch distribution over radius, C_P – blade surface pressure coefficient, k – balance coefficient for two-parameter optimization procedure, f – camber of cylinder blade sections, J_{S0} and K_{T0} – design internal advance ratio and thrust coefficient.

The choice of objective function depends on specific practical requirements regarding blading system. The most common case is the requirement to obtain the maximum efficiency of blading system η; however, other optimization criteria are also possible. The requirement may be to delay, e.g., propeller blade cavitation as much as possible, and in this case, the cavitation number σ is to be minimized. The optimum point may also be specified in terms of blade strength, levels of force and pressure fluctuations. It is also possible to have mixed optimization criteria when the blading system should be a trade-off between a number of parameters. In this paper, two-parameter optimization is considered, viz., traditional requirement of maximum propeller efficiency and, simultaneously, minimization of pressure reduction on blade surface. The unknown blade geometry parameter is distribution of pitch H over radius r. There is no cylindrical blade section camber in this problem f=0.

For optimization of propeller efficiency combined with good cavitation performance, one should set k≠0 (within the first or even second decimal places). Under this approach the optimization is primarily focused on the efficiency, while among propeller geometry options with close efficiency values the preference is given to the case with the smallest pressure reduction. If we set k=0, then the propeller is designed for the optimum efficiency but without consideration of optimum pressure reduction parameter.

The first constraint in (3) is the condition which governs the propeller operating mode. In our case, the thrust coefficient K_{T0} is assumed for operating advance ratio J_{S0}.

In solving problem (3), one may face with the situations when the blade geometry considered for the current pitch involves a danger of blades intersection. For avoiding such situations, the minimum allowable pitch H_{min} is to be prescribed. This requirement is the second constraint in (3).

For direct numerical solution of problem (3) it is reduced to the problem of mathematic programming with finite number of unknowns. For this purpose, the sought function H(r) is represented as a linear combination of basic functions:

$$H(r)=\sum_{k=1}^{N}A_k\cdot H_k(r) \quad (4)$$

The basic functions $H_k(r)$ are given a priori, and only their coefficients A_k are sought. Thus, the initial problem (3) in infinite-dimensional space is reduced to the problem of seeking N values of A_k, which ensure the minimum of objective function within given constraints. Such a problem can be solved using standard methods of non-linear programming. If these are applied, functions η, C_P and K_T in problem (3) are calculated at each step using prediction of propeller performance in tunnel (Vasiliev & Yakovlev 2001). The above-described approach is a simplification of axial pump design method (Yakovlev 2008) for the case of symmetric blade section outline.

3.4 Results of thruster design

In the thruster design process, it was assumed that the propeller diameter was D=0.2 m and the number of propeller revolutions was n=15 rps. Under these conditions, it was required to obtain the thrust coefficient K_T of about 0.337 at advance ratio J=0.13, i.e., near bollard-pull mode.

Based on the shape of the water channel of the thruster under design, the resistance coefficient was estimated to be ξ=0.38. In this case, the losses due to friction and flow past channel entry were taken into account. Considering that the channel has a constant radius, the required thrust was to be achieved at internal advance ratio J_{S0}=0.83.

The propeller was designed using the method described above. Thus, the optimum pitch distribution over radius was found with other blade geometry parameters given. The blade width distribution was chosen in accordance with the propeller case presented by Lebedev et al (1969). The blade thickness was initially chosen based on beam theory estimations, and then it was corrected using propeller strength estimates presented below. The blade section outline is symmetric, lens-shaped and similar to all cylinder blade sections.

Design process convergence to optimum solution is illustrated in Fig.2. In this case, the variations of efficiency and C_P were considered for coefficient values k=0 and k≠0 in (3), i.e., in the process of efficiency-based optimization without pressure reduction considerations and in the process of optimization for efficiency as well as pressure reduction minimization. The solutions obtained are compared. It is seen that at k=0 the propeller efficiency is smoothly increasing, but the pressure on blade is further reduced. In comparison with the two-

parameter optimization, the optimization based on the propeller efficiency only results in a 0.4% efficiency increment, but the penalty is a 30% extra pressure reduction on blade. In choosing the final design, it was found advisable to ensure better cavitation performance. Therefore, further consideration will be given to the geometry derived at k≠0.

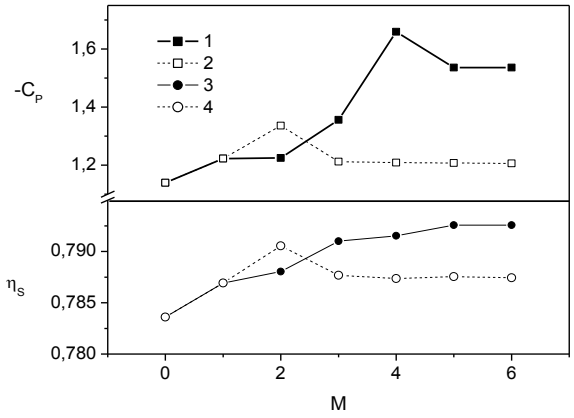

Figure 2: Convergence of propeller efficiency η_S and blade pressure reduction in the optimization process.

1 – C_P at efficiency-based optimization (k=0), 2 – C_P at optimization for efficiency and C_P (k≠0), 3 – η at efficiency-based optimization (k=0), 2 – η at optimization for efficiency and C_P (k≠0), M – number of iteration step. η_S – efficiency of propeller in pipe.

In the process of these studies, two propeller options were designed: propeller with hub (hub diameter d=0.3*D); and hubless propeller. The geometry of propellers is similar. The hubless propeller blades are different in that the thickness is reduced to internal radii and the blades are elongated.

Fig.3 shows photos of hub-type propeller and hubless propeller manufactured based on the design under consideration.

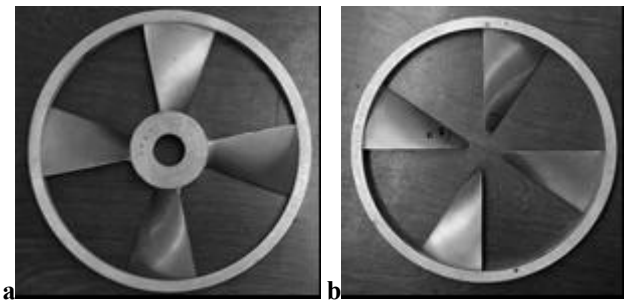

Figure 3: Models of designed propellers: hub-type design (a) and hubless design (b).

4 ADDITIONAL STUDIES ON DESIGNED PROPELLERS

Usually, propeller design is not limited to the estimations described above. After design calculations, an in-depth study of propeller performance is undertaken; first analytically and then experimentally. Based on these studies, decisions are taken on improvement of propeller design. In this case, the design was performed for research purposes and propeller adjustments were not undertaken.

4.1 Propeller blade strength study

Evaluation of propeller blade strength is an integral part of propeller design process. At present, the blade strength analysis is performed using FEM-based techniques. This type of approach to the propeller strength analysis (Volkov & Postnov 1990) has proved to be efficient for a number of full-scale structures. The calculation procedure (Volkov & Postnov 1990) intended for conventional type of propellers was modified to cover the case of RIM-driven propeller. However, these modifications have not altered the principles of this method.

For illustration of a typical stress distribution pattern for propeller blades, Fig.4 gives distributions of equivalent stresses in blades fixed in hub only, in rim only and both in hub and rim. The first case is a conventional propeller; two other cases refer to RIM-driven hubless propeller and hub-type propeller. The thickness distribution over the blade radius for this case is assumed to feature smooth increase in thickness around fixing location.

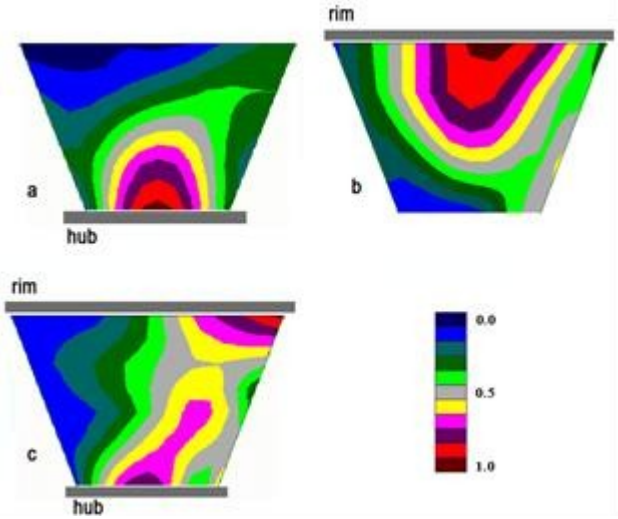

Figure 4: Blade stress distributions for the cases when blades are fixed in hub (a), in rim (b) and both in hub and rim (c). Level lines correspond to fractions of maximum stresses in each case.

As indicated by the obtained stress distributions, the area of maximum stresses is expected to shift to the areas around the blade joints. However, it should be noted that if the thickness of a rim-fixed blade is reduced, the maximum stress location may shift to the blade middle radii.

If the blade is fixed at both sides, the maximum stresses are reached near the hub and rim, but on different sides of the blade. In this case, the maximum stress location is found to be shifted to the leading edge.

The peak stresses in case of traditional hub-type design are 1.5 times higher than in the case of rim-fixed blades. Reduction of stress levels is achieved not only because of wider blade tip sections, but also due to specific load

distributions over propeller blade. Rim-fixed blades feature shorter arms of forces applied to tip sections and longer arms of forces applied to root sections. Since the loads on tip sections are usually much higher than the loads on root sections, the bending moment in the case of rim-fixed blades prove to be less than in the case of hub-fixed blades.

Stresses are reduced dramatically when blades are fixed both to hub and rim. In this case, the stress values are about 1/4 of the stress values observed for the rim-fixed blades.

Thus, the fixing arrangement in RIM-driven propellers makes it possible to reduce the propeller weight and increase propeller efficiency by using blades of reduced thickness.

4.2 Analysis of propeller cavitation performance

Fig.5 provides examples of propeller blade cavitation predictions. Calculations were done for the cavitation number σ_n=3.0:

$$\sigma_n = 2\frac{p - p_v}{\rho n^2 D^2} \qquad (5)$$

where p_v – saturated vapor pressure.

It can be seen that the propeller designed with due account of blade pressure distribution (at k≠0 in Eq. (3)), features a relatively narrow cavitation area extending along the leading edge. While the propeller designed only for optimum efficiency (at k=0 in Eq. (3)) features a wide cavitation area at tip radii, which may result in an earlier fall-off of propeller curves.

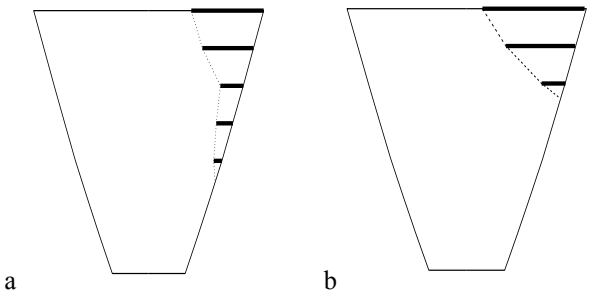

a b

Figure 5: Predicted cavitation areas for propeller blades.

a – propeller optimized for k≠0,

b – propeller optimized for k=0.

5 EXPERIMENTAL SETUP

The purpose of the tests was to analyze and compare the main characteristics of hub propeller and hubless propeller used in RIM-driven thrusters as well as to check the method of design applied for propellers of this type.

Two rim propellers with were manufactured (see Fig. 3) with a pipe section to model the channel where the thruster propeller is operating. The tests were performed in the deep-water towing tank of the Krylov Shipbuilding Research Institute. Propeller revolutions, thrust and torque were measured. The forces generated on the pipe were not measured in these tests. In case of the hub-type design, the propeller hub was connected to the dynamometer and the propeller thrust and torque was transmitted to the dynamometer via hub (see Fig.6). For testing the hubless propeller, a special-purpose strut was made to connect the rim of hubless propeller to the dynamometer shaft and transmit the thrust and torque (see Fig.7). Fig.8 shows a general view of the tested model at the test rig. The model represents a hubless propeller.

Figure 6: Propeller hub/dynamometer connection.

Figure 7: Propeller rim/dynamometer connection.

The advance ratio was varied during the hydrodynamic tests (in the full range of advance ratio values) by changing the towing speed V. The propellers were tested in the range of $0 \le J \le 1.2$, corresponding to the speed range of 0 to 3.6 m/s. For avoiding the wave-making effects in open water conditions, the propeller and duct were immersed to the depth equal to two propeller diameters as measured from the propeller axis to water surface.

In open-water tests, it is required to measure the thrust and torque generated on propeller blades only, since the size and shape of the hub and rim depend on the specific thruster design and will be different for different ships. When these components were manufactured for tests, their dimensions were also chosen with a view to structural considerations. In tests, the hub and rim are treated as integral part of hub-type propeller. For a proper account of forces and moments arising on these structures, a

dummy hub and a dummy rim were manufactured to model the shape of the real hub and rim. Prior to propeller tests, the force and moments on propellers were measured experimentally and then deducted from the force and moments generated on the propeller outfitted with hub and rim. Thus, the force and torque arising only on blades were determined. A similar method was used for hubless propeller tests, but in that case the strut and dummy rim (instead of dummy hub and dummy rim) were examined. For this test method, it is essential to take into account the force and moment on strut, because the strut is used only in tests and it does not exist in the real thruster.

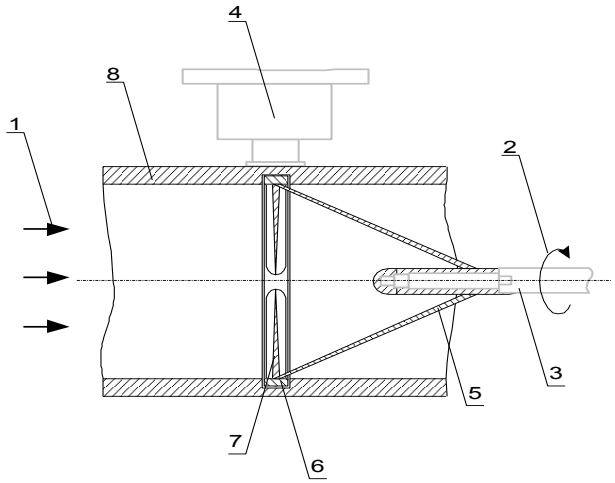

Figure 8: General view of test model setup.

1 – inflow velocity, 2 – shaft rotation, 3 – dynamometer shaft, 4 – structural component of the test rig, 5 – bracket, 6 – rim, 7 – blades of hubless propeller.

In the process of the tests, the dynamic and kinematic parameters obtained by direct measurements were used to calculate non-dimensional thrust, torque and efficiency factors. These factors were treated as functions of advance ratio J.

6 TEST RESULTS AND ANALYSIS

The relations of propeller thrust, torque and efficiency factors versus advance ratio are compared with estimated relations. This comparison is performed for hub propeller and hubless propeller designs (Fig. 9-11).

It should be noted that the presented results refer to the propeller blading system and do not include forces on pipe and hub or moment induced by rim. Advance ratio J corresponds to propulsor advance.

In general, the estimates compare fairly well with the experimental data for moderate loads. Some discrepancies are observed at small advance ratios in particular for the torque coefficient K_Q. For the propeller efficiency there is a good agreement between estimates and experiments with some overestimate of maximum values. The discrepancies between estimations and experimental data can be put down to calculation inaccuracy as well as uncertainty in assessment of moment on rim. Final conclusions can be obtained after further studies.

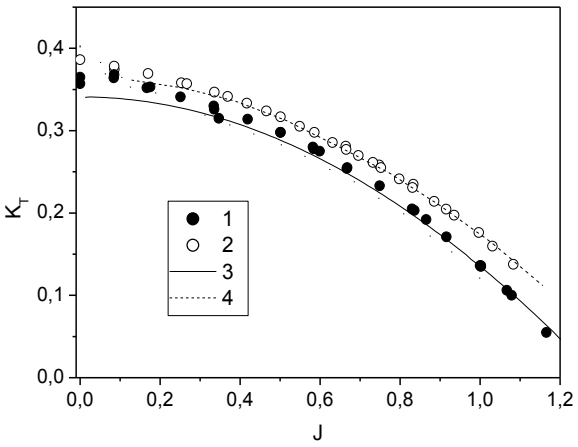

Figure 9: Analytical and experimental relations of propeller thrust coefficient versus advance ratio.

1 – experimental data for hub propeller, 2 – experimental data for hubless propeller, 3 – calculations for hub propeller, 4 – calculations for hubless propeller.

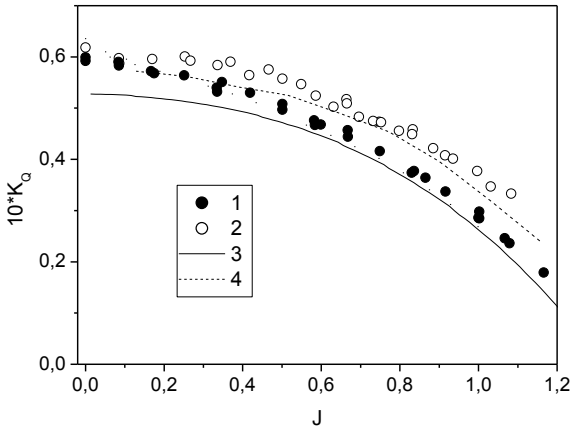

Figure 10: Analytical and experimental relations of propeller torque coefficient versus advance ratio.

Symbols as per Fig. 9

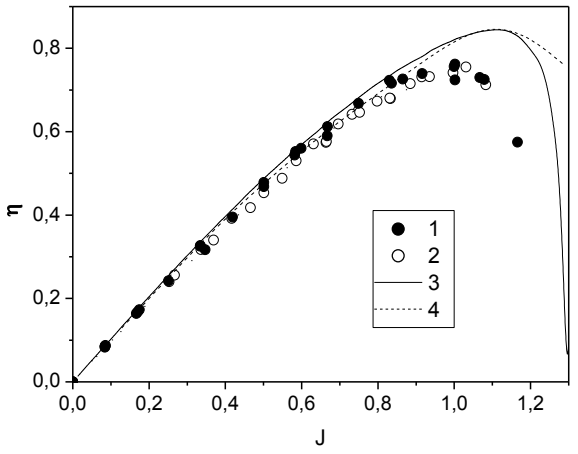

Figure 11: Analytical and experimental relations of propeller efficiency versus advance ratio.

Symbols as per Fig. 9

Comparison of data for hub propeller and hubless propeller indicate that the efficiency curves are similar, but hubless propeller has higher thrust and torque as compared to hub propeller. The latter is due to the fact that in the hubless case, there is a small reduction of the flow velocity through the propeller disk and the radial size of blades is larger.

7 CONCLUSIONS

In the process of this investigation, a hub propeller and a hubless propeller were designed as options for the RIM-driven thruster. Blade strength and cavitation characteristics were estimated for these propellers. Experimental relations of thrust and torque of propeller blading system versus advance ratio were obtained. Special-purpose measurement procedures as well as accessory equipments were developed for these experimental studies.

Based on the results of the studies the following conclusions can be drawn:

- The design method presented here for the RIM-driven thruster, including propeller blading system design, makes it possible to achieve the required thruster performance.
- The test rig developed for measuring the forces and moment on RIM-driven propeller meets the formulated requirements and proves to be suitable for experimental investigation of hub and hubless propellers.
- The conducted analytical and experimental studies identified the ways for improvement of design methods for RIM-driven thrusters.

REFERENCES

Idelchik, I. E. (ed.) (1992). Handbook on hydraulic resistance. Mashinostroenie.

Kinnas, S. A., Chang S.-H., He, L. & Johannessen, J. T. (2009). 'Performance prediction of a cavitating RIM driven tunnel thruster'. First International Symposium on Marine Propulsors. SMP'09, Trondheim, Norway.

Kulikov, S. V. & Khramkin, M. F. (1965). Waterjet propulsors (theory and design). Sudostroenie.

Lebedev, E. L., Pershitz, R. Y., Rusetskiy, A. A., Avrashkov, N. S. & Tarasyuk, A. B. (1969). Ship steering units. Sudostroenie.

Papir, A. N. (1970). Waterjet propulsors of small craft. Sudostroenie.

Rusetskiy, A. A & Mavlyudov, M. A. (2009). Waterjet propulsors. Krylov Shipbuilding Research Institute, St.Petersburg.

Vasiliev, A.V. & Yakovlev, A. Yu. (2001). 'Analytical method for estimation of axial pump hydrodynamic characteristics'. Summaries of Papers presented at XL Krylov Readings, pp.69-71, St. Petersburg, Russia.

Volkov, Yu.A. & Postnov, B.A. (1990). 'Determination of stressed-strained state of blades with complex geometry using finite element method'. Proceedings of XV All-Union Conference on shell and plate theory, Izdatelstvo Kazanskogo Universiteta.

Yakovlev, A. Yu. (2008). 'Design of blading systems by direct optimization'. Proceedings of the Krylov Shipbuilding Research Institute **35**, pp. 111-121.